Johann Radon Institute for
Computational and Applied Mathematics
Austrian Academy of Sciences (ÖAW)

A matching of singularities in domain decomposition methods for reaction-diffusion problems

C. Chniti

RICAM-Report 2008-13

A matching of singularities in domain decomposition methods for reaction-diffusion problems

Chokri Chniti
RICAM, Austrian Academy of Sciences,
Altenberger strasse 69, 4040 Linz, Austria

Abstract: In this paper the author certifies that the same approach proposed in previous works [5, 6] can be applied to more general operators than the Laplacian. We consider here the case of reaction-diffusion problems with piecewise constant coefficients. The problem reduces to determining the coefficients of some transmission boundary conditions to obtain fast convergence of domain decomposition methods. After explaining the theoretical results, we explicitly compute the coefficients in the transmission boundary conditions. The numerical results presented in this paper confirm the optimality properties.

1 Introduction

In this paper we consider the elliptic equation with highly jumping coefficients

$$\begin{cases} -\nabla.(\nu(x)\nabla u) + \eta(x)u &= f \ \text{ in } \Omega \subset \mathbb{R}^2 \\ u &= 0 \text{ on } \gamma \\ \frac{\partial u}{\partial n} &= g \text{ on } \partial\Omega \setminus \gamma\,, \end{cases} \tag{1}$$

where $\gamma \subset \partial\Omega$ corresponds to the piece of the boundary with the Dirichlet boundary condition. This equation is used for numerical modeling of the so-called skin problem. To simplify the model we choose Ω as a fragment with one cell with a lipid layer, (see Figure 1). In this paper we consider this problem with the domain Ω decomposed into two subdomains, and we restrict our attention to the case where $\gamma = \partial\Omega$. For large numerical computations with these problems, domain decomposition is a natural idea; a non-overlapping decomposition being directly induced by the different materials. We study in this paper the influence of the transmission conditions on the Schwarz algorithm for reaction-diffusion problems. We numerically test improved transmission conditions with second-order tangential derivatives, which were derived from an asymptotic analysis of the Schwarz algorithm near the corners of the domain. The theoretical optimality of the asymptotic analysis relying on the matching of the main singularities within Kondratiev's theory [3] is supported by the

numerical computations. The article is organized as follows. In Section 2, we introduce the model problem and the interface boundary condition used in this paper. In Section 3, a general form of a posteriori estimate is given. In Section 4, a rapid review of some consequences of Kondratiev's theory [3] is presented. In Section 5, we recall the strategy of improving the convergence rates around corner singularities and derive an optimal choice of the transmission conditions near the corner. In the remainder of the paper, we give some practical examples and numerical experiments which confirm the optimality of such coefficients.

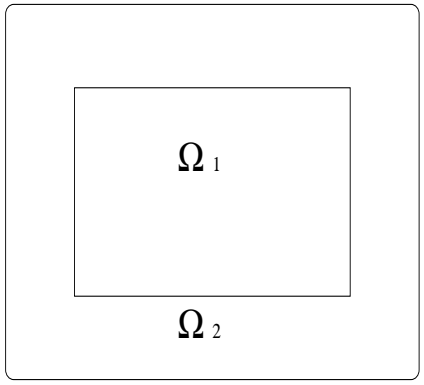

Figure 1: A skin fragment consisting of one cell (Ω_1) and lipid layer (Ω_2). $\nu(x) = \nu_1$ inside the cell and $\nu(x) = \nu_2$ in the lipid layer, with $\nu_1 << \nu_2$.

2 New interface conditions

Valid interface conditions in the vicinity of the corners are deduced from regular interfaces conditions (case without corners). We recall some results of the regular cases, and propose new interface conditions valid near the corner.

2.1 Case of a regular interface

We consider the case of reaction-diffusion problems:

$$\left\{ \begin{array}{rl} -\nabla.(\nu(x)\nabla u) + \eta(x)u & = f \quad \text{for } x \in \Omega \subset \mathbb{R}^2 \\ |u| & < +\infty \text{ as } x \to \infty\,, \end{array} \right. \tag{2}$$

where f is the right-hand side, and the scalar diffusion coefficient $\nu(x)$ and $\eta(x)$ are the piecewise constant coefficients

$$\nu(x) = \left\{ \begin{array}{l} \nu_1 \text{ in } \Omega_1 \\ \nu_2 \text{ in } \Omega_2 \end{array} \right. \qquad \eta(x) = \left\{ \begin{array}{l} \eta_1 \text{ in } \Omega_1 \\ \eta_2 \text{ in } \Omega_2 \end{array} \right. .$$

We consider here the model problem posed on the infinite plane $\Omega = \mathbb{R}^2_{xy}$. It can be decomposed into two half-planes, $\Omega_1 = (-\infty, 0) \times \mathbb{R}$ and $\Omega_2 = (0, +\infty) \times \mathbb{R}$. The solution u must satisfy two conditions at the interface $x = 0$:

$$u(0^+, y) = u(0^-, y), \text{ and } \quad \nu_1 \frac{\partial u}{\partial x}(0^+, y) = \nu_2 \frac{\partial u}{\partial x}(0^-, y), \quad y \in \mathbb{R}\,.$$

These conditions are simply the continuity of u and of the flux. We wish to analyze the performance of the Schwarz iteration [4]: If (u_1^n, u_2^n) are known, the step $n+1$ is determined by solving

$$\left\{ \begin{array}{rl} -\nu_1 \Delta u_1^{n+1} + \eta_1 u_1^{n+1} & = f \quad \text{in} \quad \Omega_1 \\ (\nu_1 \frac{\partial}{\partial n_1} + \mathcal{S}_2) u_1^{n+1}(0, y) & = (-\nu_2 \frac{\partial}{\partial n_2} + \mathcal{S}_2) u_2^n(0, y), \quad y \in \mathbb{R} \\ |u_1^{n+1}| & < \infty, \end{array} \right. \tag{3}$$

$$\left\{ \begin{array}{rl} -\nu_2 \Delta u_2^{n+1} + \eta_2 u_2^{n+1} & = f \quad \text{in} \quad \Omega_2 \\ (\nu_2 \frac{\partial}{\partial n_2} + \mathcal{S}_1) u_2^{n+1}(0, y) & = (-\nu_1 \frac{\partial}{\partial n_1} + \mathcal{S}_1) u_1^n(0, y), \quad y \in \mathbb{R} \\ |u_2^{n+1}| & < \infty, \end{array} \right. \tag{4}$$

where $\mathcal{S}_j$, $j = 1, 2$, are linear operators acting in the y direction only. By linearity, it will be sufficient to consider only the homogeneous case $f = 0$. Our simple model problem allows us to use a Fourier transform in the y variable, i.e.:

$$\hat{u}(x, k) = \int_{-\infty}^{+\infty} u(x, y) e^{-iyk} dy$$

to analyze the convergence of the Schwarz method (3) and (4). A natural question is how to choose the transmission conditions in the Schwarz method to get fast convergence of the iteration. Good choices of the transmission conditions optimize the performance of the Schwarz iteration. The main idea is to fix a certain class of local transmission conditions and to optimize the convergence factor of the iteration over this class. To do this, we need to have an explicit expression for the convergence factor ρ, although it is hard to estimate in general. For the reaction-diffusion problems, the convergence can be fully analyzed, and a convergence factor $\rho(k)$ (as a function of the frequencies tangent to the interface) can be obtained using a Fourier transform. This strategy was first introduced in [12] for the advection-diffusion equation, where a certain subclass of second order conditions was optimized for non-overlapping subdomains. By requiring that the solution in each subdomain be bounded at infinity, and applying the transmission conditions that couple the two subdomains, we find the convergence factor

$$\rho(k) = \left| \frac{\sigma_2(k) - \nu_2 \sqrt{k^2 + c_2}}{\sigma_2(k) + \nu_1 \sqrt{k^2 + c_1}} \quad \frac{\sigma_1(k) - \nu_1 \sqrt{k^2 + c_1}}{\sigma_1(k) + \nu_2 \sqrt{k^2 + c_2}} \right|$$

where $c_i = \frac{\eta_i}{\nu_i}$ and $\sigma_j(k)$ are the Fourier symbols of the operators $\mathcal{S}_j$. The practically used and efficient interface boundary conditions involve the second order tangential derivative

$$\mathcal{S}_j = \nu_j \left(\beta - \frac{\partial}{\partial \tau} (\frac{\alpha}{2} \frac{\partial}{\partial \tau}) \right),$$

where $\dfrac{\partial}{\partial \tau}$ denotes the tangential derivative and α and β are constants. A simple computation gives

$$\sigma_j(k) = \nu_j(\beta + \frac{\alpha}{2} k^2).$$

Let h is the characteristic mesh size of the numerical discretization. Assuming Ω is splited into two half-planes and for a given bounded set of frequencies in the tangential variable, proportional to $\frac{1}{h}$, there is an optimal choice of (α, β) for the convergence of the domain decomposition process (3)-(4). By introducing the error $e_i^n(x,\tau) = u_i^n - u$ at step n and its Fourier transform $\widehat{e_i^n}(x,k)$ in the tangential variable, the optimized coefficients $\alpha_{opt} > 0$ and $\beta_{opt} > 0$ are determined according to [7] by the min-max problem

$$\min_{\alpha>0, \beta \geq 0} \max_{0<k_1 \leq k \leq \frac{\pi}{h}} |\rho(k; \alpha, \beta)|, \tag{5}$$

here h is a small parameter and the convergence factor is

$$\rho(k;\alpha,\beta) = \left| \frac{\beta + \frac{\alpha}{2}k^2 - \sqrt{k^2 + c_2}}{\beta + \frac{\alpha}{2}k^2 + \frac{1}{\lambda}\sqrt{k^2 + c_1}} \quad \frac{\beta + \frac{\alpha}{2}k^2 - \sqrt{k^2 + c_1}}{\beta + \frac{\alpha}{2}k^2 + \lambda\sqrt{k^2 + c_2}} \right|$$

where $\lambda = \frac{\nu_2}{\nu_1}$.

Theorem 2.1. *(cf.[7]) The min-max problem (5) has a unique solution given by:*

$$k^\star = \sqrt{\frac{\pi}{\lambda+1}(\lambda\sqrt{k_1^2 + c_1} + \sqrt{k_1^2 + c_2})} \quad h^{-\frac{1}{2}},$$

$$\beta_{opt} = \left[\frac{\pi}{4(\lambda+1)^3} \left(\lambda\sqrt{k_1^2 + c_1} + \sqrt{k_1^2 + c_2} \right)^3 \right]^{\frac{1}{4}} \quad h^{-\frac{1}{4}},$$

and

$$\alpha_{opt} = 2 \left[\frac{\lambda+1}{4\pi^3 \left(\lambda\sqrt{k_1^2 + c_1} + \sqrt{k_1^2 + c_2} \right)} \right]^{\frac{1}{4}} \quad h^{\frac{3}{4}}.$$

After this presentation of some results in the case of regular interface, our goal now is to give the form of boundary interface conditions available near the corner and their optimal parameters.

2.2 Interface conditions in the vicinity of the corner

The decomposition of a regular domain into non-overlapping subdomains can produce interior artificial corners on the interfaces. This makes artificial singularities appear in the solution of the auxiliary limit problems. Here the full domain $\Omega = \mathbb{R}^2 = \mathbb{R}_+^* \times S^1 \cup \{O\}$ will be decomposed into two non-overlapping sectorial subdomains $\overline{\Omega} = \overline{\Omega_1} \cup \overline{\Omega_2}$, with $\Omega_1 = \mathbb{R}_+^* \times (\theta_-, \theta_+)$, $\Omega_2 = \mathbb{R}_+^* \times (\theta_+, \theta_- + 2\pi)$ and $\theta_+ - \theta_- \in (0, 2\pi)$. In the case of a singular domain, following the approach presented in [5] (see also the discussion in [8]), the interface condition of the regular interface must be modified in the vicinity of the corner. Indeed, one can show that asymptotically (as $r \to 0$) the interface conditions behave like Dirichlet interface conditions and do not transmit information well from one subdomain to its neighboring ones. This was considered in [8] as the explanation of a slow convergence of a domain decomposition algorithm around corners. One way to solve this problem is to force all the terms of the boundary interface operators to have the same homogeneity degree. Thus, a good candidate for the boundary conditions has the form $\pm\nu_i \frac{\partial}{r\partial\theta} + \widetilde{\mathcal{S}}_j$ where

$$\widetilde{\mathcal{S}}_j = \nu_j \left(\frac{\beta_{1,2}}{r} - \frac{\partial}{\partial r} \left(\frac{\alpha_{1,2}}{2} r \frac{\partial}{\partial r} \right) \right)$$

holds around the corner $r = 0$, with $\alpha_{1,2}$ and $\beta_{1,2}$ constant. Far from the corner, the interface boundary must keep the optimal form of the regular interface. Summing up, we take

$$B_{i,j}(\pm\nu_i \frac{\partial}{r\partial\theta} u, u) = \pm\nu_i \frac{\partial}{r\partial\theta} u + \nu_j \widetilde{\beta}_{1,2}(r) u - \nu_j \frac{\partial}{\partial r} \frac{\widetilde{\alpha}_{1,2}(r)}{2} \frac{\partial}{\partial r} u, \tag{6}$$

$$\text{with} \quad \widetilde{\alpha}_{1,2}(r) = \begin{cases} \alpha_{1,2} r & \text{if } r \le \dfrac{\alpha_{opt}}{\alpha_{1,2}} \\ \alpha_{opt} & \text{if } r \ge \dfrac{\alpha_{opt}}{\alpha_{1,2}} \end{cases} \qquad \widetilde{\beta}_{1,2}(r) = \begin{cases} \dfrac{\beta_{1,2}}{r} & \text{if } r \le \dfrac{\beta_{1,2}}{\beta_{opt}} \\ \beta_{opt} & \text{if } r \ge \dfrac{\beta_{1,2}}{\beta_{opt}} \end{cases}, \tag{7}$$

where $\alpha_{1,2} > 0$ and $\beta_{1,2} \ge 0$.

In the next sections, we will see how to choose α_1, β_1 in (7) in order to reduce the corner singularities of u_1^n (the same can be done for u_2^n), which is a solution of

$$\begin{cases} -\nu_1 \frac{1}{r^2} \left((r\partial_r)^2 + \partial_\theta^2 \right) u_1^{n+1}(r,\theta) + \eta_1 u_1^{n+1}(r,\theta) &= 0 \\ \left(-\nu_1 \frac{1}{r} \partial_\theta + \widetilde{\mathcal{S}}_2 \right) u_1^{n+1}(r,\theta_-) &= \left(-\nu_2 \frac{1}{r} \partial_\theta + \widetilde{\mathcal{S}}_2 \right) u_2^n(r,\theta_- + 2\pi) \\ \left(\nu_1 \frac{1}{r} \partial_\theta + \widetilde{\mathcal{S}}_2 \right) u_1^{n+1}(r,\theta_+) &= \left(\nu_2 \frac{1}{r} \partial_\theta + \widetilde{\mathcal{S}}_2 \right) u_2^n(r,\theta_+) \end{cases} . \tag{8}$$

3 A general form of a posteriori estimate

We recall the general presentation in [1, 2]. Let $\mathcal{V}$ be a reflexive Banach space and

$$J(v) := \mathcal{G}(\Lambda v) + \mathcal{F}(v), \quad \forall v \in \mathcal{V}$$

where $\mathcal{G}$ and $\mathcal{F}$ are convex continuous functionals, and Λ is a linear continuous operator that maps $\mathcal{V}$ to another Banach space Y. We assume that

$$||\Lambda w|| \geq c_1 ||w||_{\mathcal{V}}, \forall v \in \mathcal{V}\,,$$

and J is coercive on $\mathcal{V}$. The space $\mathcal{V}$ has a topologically dual counterpart $\mathcal{V}^*$. The product of $v^* \in \mathcal{V}^*$ and $v \in \mathcal{V}$ is denoted by $< v^*, v >$. The operator $\Lambda^* : \mathcal{V}^* \to Y^*$ satisfying the relation

$$(y^*, \Lambda w) =< \Lambda^* y^*, w >, \quad \forall w \in \mathcal{V},$$

is conjugate to Λ. Here (y^*, y) denotes the value of a functional $y^* \in \mathcal{V}$ on $y \in Y$. We denote by $\mathcal{G}^*$ the Fenchel conjugate of $\mathcal{G}$,i.e.,

$$\mathcal{G}^*(y^*) = \sup_{y \in Y}((y^*, y) - \mathcal{G}(y)))\,.$$

We say that $\mathcal{G}$ and $\mathcal{G}^*$ are uniformly convex in the balls $B(0, \delta) \in Y$ and $B(0, \delta^*) \in Y^*$ respectively, if they satisfy the relations

$$\mathcal{G}(\frac{y_1 + y_2}{2}) + \Gamma_\delta(\frac{y_1 - y_2}{2}) \leq \frac{1}{2}(\mathcal{G}(y_1) + \mathcal{G}(y_2))$$

$$\mathcal{G}^*(\frac{y_1^* + y_2^*}{2}) + \Gamma_{\delta^*}^*(\frac{y_1^* - y_2^*}{2}) \leq \frac{1}{2}(\mathcal{G}^*(y_1^*) + \mathcal{G}^*(y_2^*)),$$

where $\Gamma_\delta : \mathcal{V} \to \mathbb{R}_+$ and $\Gamma_{\delta^*}^* : Y^* \to \mathbb{R}_+$ are certain nonnegative functionals vanishing at zero. The theorem below gives the general form of the functional type a posteriori error majorant. It gives an upper bound of the difference $u - v$, where v is an approximate solution of our problem (for the primal problem) and $y^* - p^*$ for the dual problem.

Theorem 3.1 ([1],[2]). *Let u be a minimizer of the problem $\inf_{v \in \mathcal{V}} J(v)$, the functionals $\mathcal{F}$ and $\mathcal{G}$ satisfy the above conditions, and $\Lambda u \in B(0, \delta)$ and $p^* \in B(0, \delta^*)$. Then for any $v \in \mathcal{V}$ and $y^* \in Y^*$ such that $\Lambda v \in B(0, \delta)$ and $y^* \in B(0, \delta^*)$, the estimate*

$$\Gamma_\delta(\frac{\Lambda(v - u)}{2}) + \Gamma_{\delta^*}^*(\frac{(y^* - p^*)}{2}) \leq \mathcal{H}(v, y^*) \tag{9}$$

holds where

$$2\mathcal{H}(v,y^*) := [\mathcal{F}(v) + \mathcal{F}^*(-\Lambda^* y^*) + < \Lambda^* y^*, v >] + [\mathcal{G}(\Lambda v) + \mathcal{G}^*(y^*) - (y^*, y)] \,.$$

Here, we will apply the above general estimate to reaction-diffusion problems with our interface boundary condition. Consider the variational problem for the functional

$$J(v) = \frac{1}{2}\int_\Omega |\nabla v|^2 + \delta |v|^2 + \int_{\partial\Omega_2} (\beta |v|^2 + \frac{\alpha}{4}|\partial_\tau v|^2 - gv) ds \,.$$

The minimizer u of this variational problem is solution of

$$\left\{ \begin{array}{ccc} -\Delta u + \delta u & = 0 & \text{in } \Omega \\ \frac{\partial u}{\partial n} + \beta u - \frac{\alpha}{2}\frac{\partial^2 u}{\partial \tau^2} & = g & \text{on } \partial\Omega_2 \\ u & = 0 & \text{on } \partial\Omega_1 \end{array} \right.$$

where $\{\partial\Omega_1, \partial\Omega_2\}$ represents a partition of the boundary $\partial\Omega$. If Λ is associated with the operator ∇v, the functional a posteriori estimate for this problem is a special case of (9). Let us denote by

$$\mathcal{G}(\Lambda v) = \frac{1}{2}\int_\Omega |\nabla v|^2, \quad \mathcal{F}(v) = \int_\Omega \frac{\delta}{2}|v|^2 + \int_{\partial\Omega_2} (\beta |v|^2 + \frac{\alpha}{4}|\partial_\tau v|^2 - gv) ds \,.$$

Since

$$\int_\Omega y^*.\nabla v = \int_\Omega -\mathrm{div} y^* v + \int_{\partial\Omega_2} (y^* n) v \, ds, \quad \forall v \in V_0 \subset H^1(\Omega),$$

we observe that

$$\Lambda^* y^* = \{-\mathrm{div} y^* | \Omega, \quad y^* n | \partial\Omega_2\}.$$

In this case,

$$< y^*, y > := \int_\Omega y^*.y dx, \quad \mathcal{G}^*(-y^*) = \int_\Omega \frac{1}{2}|y^*|^2 dx \,.$$

Therefore

$$\mathcal{G}(\Lambda v) + \mathcal{G}^*(-y^*) + < y^*, \Lambda v > = \int_\Omega (\frac{1}{2}|\nabla v|^2 + \frac{1}{2}|y^*|^2 + \nabla v.y^*) dx = \int_\Omega \frac{1}{2}|\nabla v + y^*|^2 dx \,.$$

If y^* is sufficiently regular, then

$$< \Lambda^* y^*, v > = \int_\Omega -\mathrm{div} y^* v + \int_{\partial\Omega_2} (y^* n) v ds \,.$$

$$\begin{aligned} \mathcal{F}^*(\Lambda^* y^*) \quad &= \sup_{v \in V_0} \left\{ \int_\Omega -\mathrm{div} y^* v + \int_{\partial\Omega_2} (y^* n) v ds - \mathcal{F}(v) \right\} \\ &\leq \sup_{v \in H^1(\partial\Omega_2)} \int_\Omega (-\mathrm{div} y^* v - \frac{\delta}{2}|v|^2) dx + \sup_{w \in H^1(\partial\Omega_2)} \int_{\partial\Omega_2} ((y^*.n)w - \beta |w|^2 - \frac{\alpha}{4}|\partial_\tau w|^2 + gw) ds \\ &= \int_\Omega \frac{1}{2\delta}|\mathrm{div} y^*|^2 dx + \sup_{w \in H^1(\partial\Omega_2)} \int_{\partial\Omega_2} ((y^*.n)w - \beta |w|^2 - \frac{\alpha}{4}|\partial_\tau w|^2 + gw) ds \\ &\leq \int_\Omega \frac{1}{2\delta}|\mathrm{div} y^*|^2 dx + \min_{w \in H^1(\partial\Omega_2)} \int_{\partial\Omega_2} (\frac{\alpha}{4}|\partial_\tau w|^2 + \beta |w|^2 - (y^*.n)w - gw) ds \,. \end{aligned}$$

The L^2-norm of $\partial_\tau w$ is bounded by a constant M. Therefore, we get

$$\begin{aligned}
\mathcal{F}^*(\Lambda^* y^*) \quad &\leq \int_\Omega \frac{1}{2\delta}|\mathrm{div} y^*|^2 dx + \frac{\alpha}{4} M|\partial\Omega_2| + \min_{w\in H^1(\partial\Omega_2)} \int_{\partial\Omega_2} (\beta|w|^2 - (y^*.n)w - gw) ds \\
&\leq \int_\Omega \frac{1}{2\delta}|\mathrm{div} y^*|^2 dx + \frac{\alpha}{4} M|\partial\Omega_2| + \max_{w\in L^2(\partial\Omega_2)} \int_{\partial\Omega_2} (-\beta|w|^2 + (y^*.n)w + gw) ds \\
&\leq \int_\Omega \frac{1}{2\delta}|\mathrm{div} y^*|^2 dx + \frac{\alpha}{4} M|\partial\Omega_2| + \int_{\partial\Omega_2} \frac{1}{4\beta}|y^*.n + g|^2 ds\,.
\end{aligned}$$

We obtain

$$\begin{aligned}
\mathcal{F}(v) + \mathcal{F}^*(\Lambda y^*) - < \Lambda^* y^*, v > \quad &\leq \frac{1}{2\delta}\int_\Omega |\mathrm{div}(y^*) + \delta v|^2 + \frac{1}{4\beta}\int_{\partial\Omega_2} |(y^*.n) + g - 2\beta v|^2 \\
&\quad + \int_{\partial\Omega_2} \frac{\alpha}{2}|\partial_\tau v|^2 + \frac{\alpha}{4} M|\partial\Omega_2|\,.
\end{aligned}$$

4 Corner singularities analysis

An important ingredient for the analysis of corner singularities is the Mellin transform with respect to the radial variable, defined according to

$$\widehat{f}(z) = \mathcal{M}(f)(z) = \int_0^\infty r^{iz} f(r) \frac{dr}{r}\,.$$

Recall that

$$\mathcal{M}(ir\,\partial_r f)(z) = z\mathcal{M}(f)(z)\,. \tag{10}$$

Then the asymptotic expansion of u, with $Supp\, u \subset \{r \leq 1\}$:

$$u(r,\theta) = \sum_{k=1}^{\infty} \sum_{j=0}^{\mu_k - 1} a_{k,j} r^{-iz_k} \ln^j(r) \varphi_{k,j}(\theta)$$

can be written in terms of $\mathcal{M}u$ which is meromorphic in some upper half-complex plane by noticing that

- z_k are the poles of $\mathcal{M}u$,
- μ_k are their corresponding multiplicity,
- $\varphi_{k,j}$ encode the angular variations,
- $a_{k,j} \in \mathbb{R}$.

4.1 Expansion of a solution to the problem in Ω

The natural singularities exponent and the angular functions associated with the boundary value problem (1) are given by the next proposition.

Proposition 4.1. *Let $\Theta = \theta_+ - \theta_- - \pi$, and $\gamma = (\frac{\nu_2-\nu_1}{\nu_2+\nu_1})^2$. The complex numbers z for which (1) admits a non-trivial solution are given by $z_k = it_k$, $t_k \in \mathbb{R}$ with*

$$\sin^2(\pi t) = \gamma \sin^2(\Theta t)\,. \tag{11}$$

Proof. We note that $e = \psi e$, where ψ is a smooth function with compact support. Considering the principal part as $r \to 0$ of the problem (1) and applying the Mellin transform, we are led to consider the equation:

$$\left(\partial_\theta(\nu\,\partial_\theta) - \nu\, z^2\right)\hat{e}(z,\theta) = 0\,.$$

Here $\hat{e}(z,.)$ is an eigenfunction of the operator $K(\theta) = -\dfrac{\partial}{\partial\theta}(\nu\dfrac{\partial}{\partial\theta})$, defined on

$$\mathcal{D}(\theta) = \left\{ u \in H^1(\Omega),\, \left[\nu\frac{\partial u}{\partial\theta}\right]_{|\partial\Omega_1\cap\partial\Omega_2} = 0 \right\}$$

for the eigenvalue $-\nu\, z^2$. Moreover, $K(\theta)$ is a self-adjoint positive operator and thus $z^2 \leq 0$ and $z = it$ with $t > 0$. As $\nu(x)$ is a piecewise constant coefficient, we solve the problem in each subdomain. A simple calculation gives

$$A_i\,\cos(t\theta) + B_i\,\sin(t\theta) \text{ in } \Omega_i$$

Moreover, we impose that on the interface $\{\theta = \theta_\pm\}$ we have

$$\begin{array}{rl}
\hat{e}(t,\theta)\Big|_{\Omega_1,\theta_+} & = \hat{e}(t,\theta)\Big|_{\Omega_2,\theta_+} \\
\hat{e}(t,\theta)\Big|_{\Omega_1,\theta_-} & = \hat{e}(t,\theta)\Big|_{\Omega_2,\theta_-+2\pi} \\
\nu_1\frac{\partial}{\partial\theta}\hat{e}(t,\theta)\Big|_{\Omega_1,\theta_+} & = \nu_2\frac{\partial}{\partial\theta}\hat{e}(t,\theta)\Big|_{\Omega_2,\theta_+} \\
\nu_1\frac{\partial}{\partial\theta}\hat{e}(t,\theta)\Big|_{\Omega_1,\theta_-} & = \nu_2\frac{\partial}{\partial\theta}\hat{e}(t,\theta)\Big|_{\Omega_2,\theta_-+2\pi}
\end{array}\,. \tag{12}$$

This leads to

$$M_{\nu_1,\nu_2}(t)\begin{pmatrix} A_1 \\ B_1 \\ A_2 \\ B_2 \end{pmatrix} = 0_{\mathbb{R}^4},$$

where

$$M_{\nu_1,\nu_2}(z) = \begin{pmatrix}
\cos(t\theta_+) & \sin(t\theta_+) & -\cos(t\theta_+) & -\sin(t\theta_+) \\
\cos(t\theta_-) & \sin(t\theta_-) & -\cos(t(\theta_-+2\pi)) & -\sin\left(t(\theta_-+2\pi)\right) \\
-\nu_1\sin(t\theta_+) & \nu_1\cos(t\theta_+) & \nu_2\sin(t\theta_+) & -\nu_2\cos(t\theta_+) \\
-\nu_1\sin(t\theta_-) & \nu_1\cos(t\theta_-) & \nu_2\sin(t(\theta_-+2\pi)) & -\nu_2\cos(t(\theta_-+2\pi))
\end{pmatrix}.$$

The poles are solutions of $\det M_{\nu_1,\nu_2}(t) = 0$. A straight forward computation then gives

$$\frac{(\nu_1+\nu_2)^2}{4\nu_1\nu_2}\cos(2\pi t) - \frac{(\nu_1-\nu_2)^2}{4\nu_1\nu_2}\cos(2t(\theta_+ - \theta_- - \pi)) = 1$$

Therefore, the poles are solutions of

$$\sin^2(\pi t) = \gamma \sin^2(t(\theta_+ - \theta_- - \pi)), \tag{13}$$

where $\gamma = \left(\frac{\nu_2-\nu_1}{\nu_2+\nu_1}\right)^2$. □

Then, the first term in the asymptotic expansion of u is given by

$$e(r,\theta) = A_0 + r^{\tau_1}\begin{cases} A_1\cos(\tau_1\theta) + B_1\sin(\tau_1\theta) & \text{in } \Omega_1 \\ \\ A_2\cos(\tau_1\theta) + B_2\sin(\tau_1\theta) & \text{in } \Omega_2 \end{cases} + o(r^{\tau_1}),$$

where τ_1 denotes the first positive solution of (11).

4.2 Subproblem in Ω_1

We focus on the subdomain Ω_1, the treatment of Ω_2 being similar. The boundary problem with the selected interface conditions solved with the error $e_1^{n+1} = u_1^{n+1} - u$ reads

$$\begin{cases} -\nu_1\frac{1}{r^2}\Big((r\partial_r)^2 + \partial_\theta^2\Big)e_1^{n+1}(r,\theta) + \eta_1 e_1^{n+1}(r,\theta) & = 0 \\ \Big(-\nu_1\frac{1}{r}\partial_\theta + \widetilde{\mathcal{S}}_2\Big)e_1^{n+1}(r,\theta_-) & = \Big(-\nu_2\frac{1}{r}\partial_\theta + \widetilde{\mathcal{S}}_2\Big)e_2^{n}(r,\theta_- + 2\pi) \\ \Big(\nu_1\frac{1}{r}\partial_\theta + \widetilde{\mathcal{S}}_2\Big)e_1^{n+1}(r,\theta_+) & = \Big(\nu_2\frac{1}{r}\partial_\theta + \widetilde{\mathcal{S}}_2\Big)e_2^{n}(r,\theta_+) \end{cases}, \tag{14}$$

where

$$\widetilde{\mathcal{S}}_2 = \nu_2\left(\frac{\beta_1}{r} - \frac{\partial}{\partial r}\left(\frac{\alpha_1}{2}r\frac{\partial}{\partial r}\right)\right).$$

The case $\beta \neq 0$ is not permitted in interior corners of $\Omega = \mathbb{R}^2$, or more generally when the general solution of the complete problem does not vanish at $r = 0$ (for further details see [6]). The main singularities associated with this problem are derived following Kondratiev's theory [3]. By considering the principal part as $r \to 0$ and by applying the Mellin transform, leading to the system

$$\begin{cases} (\partial_\theta^2 - z^2)\widehat{e_1^{n+1}}(z,\theta) & = 0 \\ (\partial_\theta - \lambda\frac{\alpha_1}{2}z^2)\widehat{e_1^{n+1}}(z,\theta_-) & = \widehat{g_-^n}(z) \\ \big(\partial_\theta + \lambda\frac{\alpha_1}{2}z^2\big)\widehat{e_1^{n+1}}(z,\theta_+) & = \widehat{g_+^n}(z) \end{cases}, \tag{15}$$

where

$$\widehat{g_+^n}(z) = \lambda\left(\partial_\theta + \frac{\alpha_1}{2}z^2\right)\widehat{e_2^n}(z,\theta_+), \quad \widehat{g_-^n}(z) = \lambda(\partial_\theta - \frac{\alpha_1}{2}z^2)\widehat{e_2^n}(z,\theta_- + 2\pi), \quad \lambda = \frac{\nu_2}{\nu_1},$$

and whose solution is

$$\begin{aligned}
\widehat{e_1^{n+1}} &= a(z)e^{z(\theta-\theta_-)} + b(z)e^{-z(\theta-\theta_+)} \\
\begin{pmatrix} a(z) \\ b(z) \end{pmatrix} &= \frac{1}{z}\mathcal{R}(z)\begin{pmatrix} \widehat{g_+^n}(z) \\ \widehat{g_-^n}(z) \end{pmatrix} \\
\text{with } \mathcal{R}(z) &= \begin{pmatrix} (1+\lambda\frac{\alpha_1}{2}z)e^{z(\theta_+-\theta_-)} & -1+\lambda\frac{\alpha_1}{2}z \\ 1-\lambda\frac{\alpha_1}{2}z & -(1+\lambda\frac{\alpha_1}{2}z)e^{z(\theta_+-\theta_-)} \end{pmatrix}^{-1}.
\end{aligned}$$

Proposition 4.2. *The poles with a positive imaginary part of the factor $\mathcal{R}(z)$ are $z = it$, with*

$$\tan\left(\frac{\pi x t}{2}\right) = \frac{2}{\lambda\alpha_1 t} \tag{16}$$

$$\tan\left(\frac{\pi x t}{2}\right) = -\frac{\lambda\alpha_1}{2}t, \tag{17}$$

with $x = \frac{\theta_+-\theta_-}{\pi}$, whose positive solutions are denoted by $t_k, k \in \mathbb{N}^*$, in the increasing order.

Proof. See [6] □

The question arises: which of the equations, (16) or (17), gives the first pole?
The best way to understand which equation provides the first solution $t_1 > 0$ is the graphical representation of $t \to \tan(\frac{\pi x t}{2}), t \to \frac{2}{\lambda\alpha_1 t},$ and $t \to -\frac{\lambda\alpha_1}{2}t$, where $x = \frac{\theta_+-\theta_-}{\pi}$. It is easy to find that the first pole it_1 is associated with the equation

$$\tan\left(\frac{\pi x t}{2}\right) = \frac{2}{\lambda\alpha_1 t}\,.$$

In the next section, we derive an optimal parameter α_1 for the subproblem in Ω_1 (if it is possible) such that the first pole it_1 will be cancelled.

5 Theoretical choice of the parameters α_1

We give here a short summary of the strategy of optimization - for further details refer to [6]. Expecting that better matching yields faster convergence, our strategy to determine the "best parameter" (α_i) is the following: assuming that at step n the error functions $e_i^n = u_i^n - u$, $i = 1, 2$, have the asymptotic type of the problem on the full domain Ω, the error functions e_i^{n+1} should keep this asymptotic type up to some large enough order as $r \to 0$. (*That is, domain decomposition is used for the solution procedure, and for the corresponding iteration we try to define the transmission conditions in such a way that additional artificial singularities in the corner either are suppressed*

or are at most of the same order as the singularity of the original problem.) The analysis focuses on the first artificial pole, which is the one with the smallest imaginary part. The corresponding residue depends on the right-hand side in (8), which for the first order is given by the asymptotic type of the full domain problem. The question now becomes whether it is possible to choose the parameter α_i in Ω_i, $i = 1, 2$, so that if the data involved in the right-hand side of (8) has the right asymptotic type, then the first artificial pole is cancelled by a vanishing residue. The computation will show that such a choice of the parameter is not always possible, and in the general case we have to choose between two solutions in each subdomain Ω_i, $i = 1, 2$:

1. Check if it is possible to cancel the first artificial pole according to the previous process.

2. If the first approach has no solution, choose the parameter $\alpha_i, i = 1, 2$, in such a way that the first artificial pole has the largest possible imaginary part.

Keep in mind that $\beta_i = 0$ [1] is necessary because the solution u, has in general, a nonzero value at $r = 0$. Only the coefficients α_i can be used. In the subdomain Ω_1 and for a general right-hand side in (8), the first artificial term in the asymptotic expansion of e_1^{n+1} appears with the factor r^{t_1}, with t_1 defined in Proposition 4.2 . The first (and most efficient) approach assumes that at step n the error has the natural asymptotic type associated with the global problem:

$$e_2^n(r,\theta) = A_0 + r^{\tau_1}\left(A_2\cos(\tau_1\theta) + B_2\sin(\tau_1\theta)\right) + o(r^{\tau_1})\,.$$

With an additional truncation in $\{r \le R\}$ we set the following like in the domain decomposition algorithm

$$\begin{aligned} g_+^n(r) &= 1_{\{r\le R\}}\lambda\left(\partial_\theta - \tfrac{\alpha_1}{2}(r\partial_r)^2\right)e_2^n(r,\theta_+) \\ g_-^n(r) &= 1_{\{r\le R\}}\lambda\left(\partial_\theta + \tfrac{\alpha_1}{2}(r\partial_r)^2\right)e_2^n(r,\theta_- + 2\pi)\,, \end{aligned}$$

where $R \in \mathbb{R}_+^*$. After working with the first order expansion of the global problem, neglecting the $o(r^{\tau_1})$ remainder and taking the Mellin transform, this provides

$$\begin{aligned} \widehat{g_+^n}(z) &= \tfrac{R^{\tau_1+iz}}{\tau_1+iz}\lambda\tau_1\Big\{A_2\left(-\sin(\tau_1\theta_+) - \tau_1\tfrac{\alpha_1}{2}\cos(\tau_1\theta_+)\right) + B_2\left(\cos(\tau_1\theta_+) - \tau_1\tfrac{\alpha_1}{2}\sin(\tau_1\theta_+)\right)\Big\}, \\ \widehat{g_-^n}(z) &= \tfrac{R^{\tau_1+iz}}{\tau_1+iz}\lambda\tau_1\Big\{A_2\left(-\sin(\tau_1(\theta_- + 2\pi)) + \tau_1\tfrac{\alpha_1}{2}\cos(\tau_1(\theta_- + 2\pi))\right) \\ &\qquad + B_2\left(\cos(\tau_1(\theta_- + 2\pi)) + \tau_1\tfrac{\alpha_1}{2}\sin(\tau_1(\theta_- + 2\pi))\right)\Big\}. \end{aligned}$$

[1] Practically, the case $\beta_i = 0$ is implemented by keeping a constant coefficient $\tilde{\beta}(r) = \beta_{opt}$ along the whole interface.

We note that the boundary conditions do not contain a constant term $\left(\partial_\theta - \frac{\alpha_1}{2}(r\partial_r)^2\right)$ and therefore $g^n_\pm$ do not depend on the first term (A_0) in the expansion of e^n_2.

Our goal is to see whether there exists α_1 such that

$$\mathcal{R}(z)\begin{pmatrix} \widehat{g^n_+}(z) \\ \widehat{g^n_-}(z) \end{pmatrix} \text{ does not have any more pole on } it_1, (t_1 > 0).$$

According to [5, 6], here the cancellation of the first artificial pole it_1 is reduced to the simple condition

$$\widehat{g^n_+}(it_1) = -\widehat{g^n_-}(it_1)\,. \tag{18}$$

Proposition 5.1. *The equation (18) gives*

$$\alpha_1 = \frac{2}{\tau_1}\frac{1}{\tan(\frac{\theta_+-\theta_--2\pi}{2}\tau_1)} \text{ for } \frac{\theta_+-\theta_-}{\pi} \in (2-\frac{2}{\tau_1}, 2-\frac{1}{\tau_1})\,. \tag{19}$$

Proof. The equation (18) does not depend on the truncation parameter R and reads simply

$$\alpha_1 = \alpha_1 = \frac{2}{\tau_1}\frac{1}{\tan(\frac{\theta_+-\theta_--2\pi}{2}\tau_1)}\,.$$

We recall that $0 < \theta_+ - \theta_- < 2\pi$, which implies

$$-\pi < \frac{\theta_+-\theta_--2\pi}{2}\tau_1 < 0.$$

If $\frac{\theta_+-\theta_--2\pi}{2}\tau_1 \in (-\pi, -\frac{\pi}{2})$, then the parameter α_1 is positive and this yields the result. □

Remark 5.2. *If $\nu_1 = \nu_2$, condition (19) becomes*

$$\alpha_1 = \frac{2}{\tan(\frac{\theta_+-\theta_-}{2})} \text{ for } \frac{\theta_+-\theta_-}{\pi} \in (0,1)$$

and thus, we recover the optimized coefficients of the Laplace operator in the same domain [5, 6].

6 Examples

The characteristic equation (11) cannot be solved explicitly. Therefore, in this section we consider the usual case of calculations of neutronics $\theta_+ - \theta_- = \frac{\pi}{2}$. In this case we can explicitly compute the first pole

$$\tau_1 = \frac{1}{\pi}\arccos\left(-\quad\frac{\nu_1^2+\nu_2^2+6\nu_1\nu_2}{2(\nu_1+\nu_2)^2}\right)\,.$$

Moreover, $\tau_1 \in (\frac{2}{3}, 1)$. Then (11) yields

$$\alpha_1 = -\frac{2}{\tau_1}\frac{1}{\tan(\frac{3\pi}{4}\tau_1)} > 0\,.$$

In the case when $\theta_+ - \theta_- = \frac{3\pi}{2}$, the first pole is the same like the case where $\theta_+ - \theta_- = \frac{\pi}{2}$. But, in this case (11) gives

$$\alpha_1 = -\frac{2}{\tau_1}\frac{1}{\tan(\frac{\pi}{4}\tau_1)} < 0\,.$$

Therefore, for a given $\theta_+ - \theta_-$ we cannot always cancel the first artificiel pole, so the two strategies of optimization can be used for our problem. For instance, when the domain Ω is decomposed into one cell Ω_1 and a lipid layer Ω_2, correspond to the case of Figure 1, we see that the first strategy is used only in the cell and the second strategy in Ω_2. Up to now, we keep in mind that the first approach depending on the angle of the subdomain Ω_i, does not admit a solution in all cases. The second approach will also be tested when necessary.

If we consider the case where $\nu_1 = 1$ and $\nu_2 >> \nu_1$, then the first pole is given by

$$\tau_1 = \frac{1}{\pi}\arccos\left(-\quad\frac{1+\nu_2^2+6\nu_2}{2(1+\nu_2)^2}\right)\,.$$

According to the formula for τ_1, one sees that τ_1 is monotonically decreasing with ν_2 (we consider ν_2 as parameter) to the value $\frac{2}{3}$. Therefore, the solution of the interface problem belongs to $H^{1+\frac{2}{3}}(\Omega)$ independently of the jump discontinuity of the diffusion coefficient. We recall that the Sobolev space $H^s(\Omega)$, $s > 0, s \notin \mathbb{N}$, is defined as the space of all distributions with finite norm:

$$||v||^2_{H^s(\Omega)} = ||v||^2_{H^m(\Omega)} + \sum_{|\zeta|=m}\int_\Omega\int_\Omega \frac{|D^\zeta v(x) - D^\zeta v(y)|^2}{|x-y|^{2+2\sigma}}dxdy$$

where $s = m+\sigma$, $m \in \mathbb{N}$, $\sigma \in (0,1)$ and D^ζ denotes the derivatives with respect to the multi-index $\zeta = (\zeta_1, \zeta_2)$ (see [11] for more details).

7 Discrete problem

A direct discretization would require the computation of the normal derivatives along the interfaces $\theta_\pm$ in order to evaluate the right-hand sides in the transmission conditions in the Schwarz algorithm. At the interface $\{\theta = \theta_\pm\}$ this can be avoided by introducing four new variables

$$\begin{aligned}
\lambda^n_{(1,\theta_-)} &= \left(-\nu_2\tfrac{1}{r}\partial_\theta + \widetilde{\mathcal{S}}_2\right) u_2^n(r,\theta_-),\\
\lambda^n_{(1,\theta_+)} &= \left(\nu_2\tfrac{1}{r}\partial_\theta + \widetilde{\mathcal{S}}_2\right) u_2^n(r,\theta_+),\\
\lambda^n_{(2,\theta_-)} &= \left(\nu_1\tfrac{1}{r}\partial_\theta + \widetilde{\mathcal{S}}_1\right) u_1^n(r,\theta_-),\\
\lambda^n_{(2,\theta_+)} &= \left(-\nu_1\tfrac{1}{r}\partial_\theta + \widetilde{\mathcal{S}}_1\right) u_1^n(r,\theta_+)\,.
\end{aligned}$$

The algorithm then becomes

$$\left\{\begin{array}{rl} -\nu_1\frac{1}{r^2}\Big((r\partial_r)^2+\partial_\theta^2\Big)u_1^{n+1}(r,\theta)+\eta_1 u_1^{n+1}(r,\theta) &= 0\\ \Big(-\nu_1\frac{1}{r}\partial_\theta+\widetilde{\mathcal{S}_2}\Big)\,u_1^{n+1}(r,\theta_-) &= \lambda^n_{(1,\theta_-)}\\ \Big(\nu_1\frac{1}{r}\partial_\theta+\widetilde{\mathcal{S}_2}\Big)\,u_1^{n+1}(r,\theta_+) &= \lambda^n_{(1,\theta_+)}\\ -\nu_2\frac{1}{r^2}\Big((r\partial_r)^2+\partial_\theta^2\Big)u_2^{n+1}(r,\theta)+\eta_2 u_2^{n+1}(r,\theta) &= 0\\ \Big(\nu_2\frac{1}{r}\partial_\theta+\widetilde{\mathcal{S}_1}\Big)\,u_2^{n+1}(r,\theta_-) &= \lambda^n_{(2,\theta_-)}\\ \Big(-\nu_2\frac{1}{r}\partial_\theta+\widetilde{\mathcal{S}_1}\Big)\,u_2^{n+1}(r,\theta_+) &= \lambda^n_{(2,\theta_+)} \end{array}\right.$$

and

$$\begin{array}{rl} \lambda^{n+1}_{(1,\theta_-)} &= -\lambda^n_{(2,\theta_-)}+\Big(\nu_2\tilde{\beta}_1(r)+\nu_1\tilde{\beta}_2(r)-\partial_r(\frac{[\nu_2\tilde{\alpha}_1(r)+\nu_1\tilde{\alpha}_2(r)]}{2}\partial_r)\Big)u_2^n(r,\theta_-)\,,\\ \lambda^{n+1}_{(2,\theta_-)} &= -\lambda^n_{(1,\theta_-)}+\Big(\nu_2\tilde{\beta}_1(r)+\nu_1\tilde{\beta}_2(r)-\partial_r(\frac{[\nu_2\tilde{\alpha}_1(r)+\nu_1\tilde{\alpha}_2(r)]}{2}\partial_r)\Big)u_1^n(r,\theta_-)\,,\\ \lambda^{n+1}_{(1,\theta_+)} &= -\lambda^n_{(2,\theta_+)}+\Big(\nu_2\tilde{\beta}_1(r)+\nu_1\tilde{\beta}_2(r)-\partial_r(\frac{[\nu_2\tilde{\alpha}_1(r)+\nu_1\tilde{\alpha}_2(r)]}{2}\partial_r)\Big)u_2^n(r,\theta_+)\,,\\ \lambda^{n+1}_{(2,\theta_+)} &= -\lambda^n_{(1,\theta_+)}+\Big(\nu_2\tilde{\beta}_1(r)+\nu_1\tilde{\beta}_2(r)-\partial_r(\frac{[\nu_2\tilde{\alpha}_1(r)+\nu_1\tilde{\alpha}_2(r)]}{2}\partial_r)\Big)u_1^n(r,\theta_+)\,. \end{array} \tag{20}$$

The numerical computations with the FreeFem++ software consist in introducing the problem to be solved in each subdomain with its weak formulation. The variational formulation of the problem for each subdomain with interface conditions (6) is given by

$$\begin{aligned}\int_{\Omega_i}\eta_i\,u_i^{n+1}v_i+\int_{\Omega_i}\nu_i\nabla u_i^{n+1}\nabla v_i+\int_0^\infty\nu_j\tilde{\beta}_i(r)(u_i^{n+1}v_i)(r,\theta_\pm)+\int_0^\infty\frac{\nu_j\tilde{\alpha}_i(r)}{2}(\partial_r u_i^{n+1}\partial_r v_i)(r,\theta_\pm)\\ =\int_{\Omega_i}fv_i+\int_0^\infty\lambda^n_{(i,\theta_\pm)}v_i(r,\theta_\pm)\end{aligned}$$

and all variational formulations are discretized by a P1-Lagrange finite element method. This leads to a matrix form of the algorithm:

$$\begin{array}{rl} \widetilde{\mathcal{K}_1}u_1^{n+1} &= f+B_1^T\lambda_1^n,\\ \widetilde{\mathcal{K}_2}u_2^{n+1} &= f+B_2^T\lambda_2^n,\\ \mathcal{M}_\Gamma\lambda_1^{n+1} &= -\mathcal{M}_\Gamma\lambda_2^n+(\mathcal{M}_{\tilde{\beta}_1,\Gamma}+\mathcal{M}_{\tilde{\beta}_2,\Gamma}+\mathcal{K}_{\tilde{\alpha}_1,\Gamma}+\mathcal{K}_{\tilde{\alpha}_2,\Gamma})B_2u_2^{n+1},\\ \mathcal{M}_\Gamma\lambda_2^{n+1} &= -\mathcal{M}_\Gamma\lambda_1^n+(\mathcal{M}_{\tilde{\beta}_1,\Gamma}+\mathcal{M}_{\tilde{\beta}_2,\Gamma}+\mathcal{K}_{\tilde{\alpha}_1,\Gamma}+\mathcal{K}_{\tilde{\alpha}_2,\Gamma})B_1u_1^{n+1}, \end{array} \tag{21}$$

where λ_1,λ_2,u_1 and u_2 denote the degrees of freedom of the finite element functions approaching the solution of the continuous problem, with the same names. The matrices B_1 and B_2 are the restriction operators (entries are one or zero) corresponding to trace operators of the domains Ω_1 and Ω_2 along the interface between the two subdomains. The matrices $\widetilde{\mathcal{K}_1}$ and $\widetilde{\mathcal{K}_2}$ arise from the discretization of the Laplace subproblems with the interface conditions (6)

$$\widetilde{\mathcal{K}_j}=\eta_j\mathcal{M}_j+\mathcal{K}_j+\nu_iB_j^T(\mathcal{M}_{\tilde{\beta}_j,\Gamma}+\mathcal{K}_{\tilde{\alpha}_j,\Gamma})B_j,\quad\forall i,j=1,2,i\neq j. \tag{22}$$

Here $\mathcal{K}_1$ and $\mathcal{K}_2$ are the subdomain stiffness matrices, $\mathcal{M}_1$ and $\mathcal{M}_2$ are the subdomain mass matrices, $\mathcal{M}_\Gamma$ and $\mathcal{M}_{\tilde{\beta}_j,\Gamma}$ are the interface mass matrices, and $\mathcal{K}_{\tilde{\alpha}_j,\Gamma}$ is the interface stiffness matrix,

$$\begin{aligned}(\mathcal{M}_\Gamma)_{ij} &= \int_0^\infty (\phi_i\phi_j)(r,\theta_-)\ dr,\\ (\mathcal{M}_{\tilde{\beta}_k,\Gamma})_{ij} &= \int_0^\infty \tilde{\beta}_k(r)(\phi_i\phi_j)(r,\theta_-)\ dr,\\ (\mathcal{K}_{\tilde{\alpha}_k,\Gamma})_{ij} &= \int_0^\infty \frac{\tilde{\alpha}_k(r)}{2}(\partial_r\phi_i\partial_r\phi_j)(r,\theta_-)\ dr.\end{aligned}$$

The functions ϕ_i and ϕ_j are the basis functions associated with the degrees of freedom i and j along the interface $\{\theta = \theta-\}$.

8 Numerical results

The numerical computations with the FreeFem++ software consist in introducing the problem to be solved in each subdomain with its weak formulation. In the weak formulation of our problem, the tangential derivative involved in the boundary operator is implemented in FreeFem++ using the normal derivative (i.e. $\frac{\partial u}{\partial \tau} = \nabla u\,.\,\nu^\perp$, where ν is the normal vector and $\nu^\perp$ denotes the orthogonal of ν). All variational formulations are discretized by a P1-Lagrange finite element method. The effect of singularities associated with corners on domain decomposition methods is transparent when the discretization is fine enough. In order to show such effects without excessively increasing the numerical cost, a refinement of the mesh around the corner is considered. When the domain Ω is decomposed into two subdomains, one of them must be nonconvex. Assume $x(\Omega_1) < 1$ and $x(\Omega_2) > 1$. The first strategy can be applied in Ω_1 with the optimal choice given by (19), while choosing the coefficient α_2 to be zero or very small in Ω_2 pushes the first artificial singularity as far as possible (second strategy). With this choice, the expansion of the artificial singularities around $r = 0$ has the order $O(r^{\min(t_2(\Omega_1),t_1(\Omega_2))})$. In our comparison of numerical methods, we shall use the terminology:

1. **ICCC** for the interface conditions with constant coefficients $(\alpha_{opt}, \beta_{opt})$ up to the corner.

2. **OCC** for the new interface conditions with optimized coefficients at the corner $(\alpha_{1,2}, \beta_{1,2})$.

Figure 1 contains four interior corners. In order to have a good study of our problem one can consider a domain with only one interior corner. The simple domain which will be considered in

our computation is a disc of radius one, centered at the origin. This global domain is divided into two subdomains- Ω_1 is a quarter of a disc and $\Omega_2 = \Omega \setminus \Omega_1$, see Figure 2.

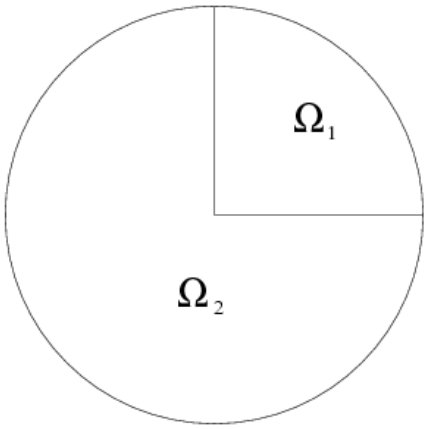

Figure 2: A disc decomposed into two sectors. $\nu(x) = \nu_1$ in Ω_1 and $\nu(x) = \nu_2$ in Ω_2 with $\nu_1 << \nu_2$.

The right-hand side f is taken constant and equal to 1 in the whole domain Ω. The convergence will be tested, and the logarithmic convergence curve will be plotted with the norm

$$|e|_1 = \left(\int_\Omega |\nabla e(x)|^2 dx \right)^{1/2}$$

A comparison of the L^∞-norm

$$\|e\|_{L^\infty(\Omega)}$$

of the error $|e_1(x)|$ was given for **OCC** and **ICCC**. Practically, the error function e^n at step n is computed as $u^N - u^n$ where u^n is the result after n iterations of the domain decomposition algorithm and N is large enough so that u^N is much closer to the (discrete) solution u^∞ than the numerical tolerance $\varepsilon = 10^{-12}$. We will show by a series of numerical results that the relation (19) is optimal, and we limit our study to the geometrical configuration with only one interior corner,

corresponding to the case of a circular domain decomposed into two subdomains. Here the disc is decomposed into two sectors with angles $\frac{\pi}{2}$ and $\frac{3\pi}{2}$. In the nonconvex subdomain Ω_2 with angle $\frac{3\pi}{2}$, the choice of $\alpha_2 = 0$ is done by taking $\widetilde{\alpha}_2(r)$ equal to 0 on five meshes of the grid by truncation. In the convex subdomain Ω_1 with angle $\frac{\pi}{2}$, we take $\alpha_1 = -\frac{2}{\tau_1}\frac{1}{\tan(\frac{3\pi}{4}\tau_1)}$, and we checked that the matching parameter $(\frac{\alpha_{opt}}{\alpha_{1,2}})$ in (7) is larger than four times the mesh size h of the refined mesh.

We use a uniform grid everywhere except at the corner $r = 0$. The domain decomposition algorithm is tested with various ratios $\dfrac{\nu_2}{\nu_1}$ in order to check that (19) is optimal (see Table 1). We recall that the abbreviation **OCC** for the optimal parameter α_1 will be compared with the **ICCC** case (constant coefficients along the interface). If we take $\dfrac{\nu_2}{\nu_1} = 2$, case where $\nu_1 = 1$ and $\nu_2 = 2$, then with **ICCC**, 22 iterations are necessary in order to reach $|e_1^n|_1 \leq 10^{-6}$ instead of 12 with **OCC**. The plot of $\log_{10}|e_1^n|_1$ with respect to n (see Figure 3) shows the improvement brought by **OCC**. Table 2 gives the L^∞-norm of the error $|e_1(x)|$ with respect to n and shows the improvement given by **OCC**.

ν_2	2	4	6	8	10	10^2	10^3	10^4	10^5	10^6
Number of iterations with **OCC**	12	10	8	8	7	7	3	3	2	1
Number of iterations with **ICCC**	22	14	11	9	8	7	3	3	2	1

Table 1: Refined mesh around the corner. Number of iterations for different values of ν_2 with $|e_1^n|_1 < 10^{-6}$.

Iteration	2	4	6	8	10	12
OCC	8.52549e-3	5.44888e-4	7.09332e-05	1.19646e-05	2.61246e-06	6.51708e-07
ICCC	8.54753e-3	4.38909e-4	7.59511e-05	2.78231e-05	1.43401e-05	8.25715e-06
$\frac{\lvert e_1^n\rvert_{\infty,\mathbf{ICCC}}}{\lvert e_1^n\rvert_{\infty,\mathbf{OCC}}} \simeq$	1.002	0.80	1.07	2.33	5.49	12.67

Table 2: The case $\nu_1 = 1, \nu_2 = 2$. Comparison of $|e_1^n|_\infty$ near the corner with **OCC** and **ICCC** with respect to the number of iterations.

9 Conclusion

All the numerical experiments show that the implementation of **OCC** method improves the behavior of the error in the decomposition algorithms. The optimal coefficients for the corresponding transmission conditions are characterized in order to reduce the singularity in the error term. Considering the results obtained in this paper, we plan in the future to tackle the following open

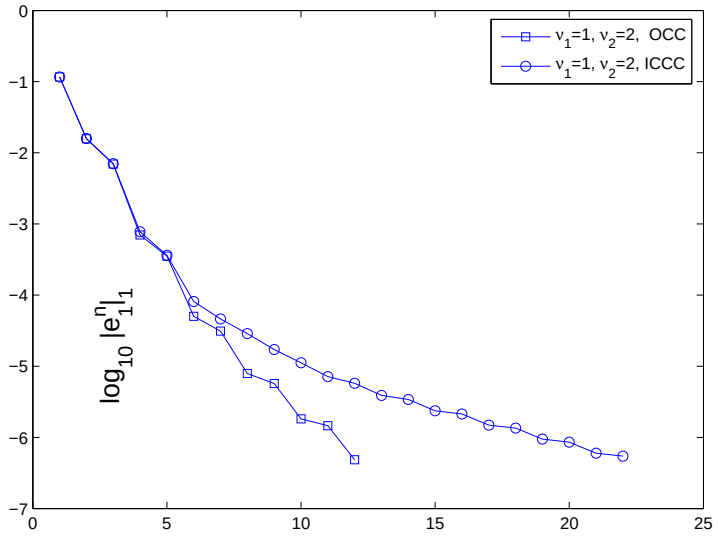

Figure 3: $\log_{10}|e_1^n|_1$ with respect to the number of iterations. The **OCC** method is represented by the clear blue squares, and the **ICCC** method is represented by the clear blue circles, with $|e_1^n|_1 < 10^{-6}$, $\nu_1 = 1$ and $\nu_2 = 2$.

questions:

- Unfortunately, there is no convergence proof that the iteration scheme converges. Nevertheless, in this paper the numerical results seem to confirm the hypothesis of convergence.
- What happens if the pole of the resolvent is of higher order?
- A good application of our methods in such situations can be observed in two-dimensional domains with more than three subdomains sharing an interior point. One can suppose that the interface in the vicinity of an interior singular point consists of two intersecting lines.
- Extension of our results to the three-dimensional case.

References

[1] S. Repin. A posteriori estimates for approximate solutions of variational problems with strongly convex functionals. Problems of Mathematical Analysis 17(1997),pp. 199-226(Russian); translation in J.Math.Sci. New York 97 (1999),pp.4311-4328.

[2] S. Repin. A posteriori error estimation for variational problems with uniformly convex functionals. Math.Comp, 69(2000), pp; 481-500.

[3] V.A. Kondratiev. Boundary problems for elliptic equations in domains with conical or angular points. Trudi Mosk. Mat. Obsc, 16, 1976, 227-313.

[4] H.A. Schwarz. Über einen Grenzübergang durch alternierendes Verfahren. Vierteljahrsschrift der Naturforschenden Gesellschaft in Zürich. Vol.15, may 1870, pp.272-286.

[5] C. Chniti, F. Nataf, F. Nier. Improved Interface Conditions for the Domain Decomposition of a Non-Convex Polygonal Domain. CRAS 342(11) (2006), pp 883-886.

[6] C. Chniti, F. Nataf, F. Nier. Improved interface condition for 2D domain decomposition with corner: a theoretical determination. Prépublication IRMAR 06-02. preprint in HAL-CCSD. http://hal.ccsd.cnrs.fr/ccsd-00018965. To appear in Calcolo.

[7] O. Dubois. Optimized Schwarz Methods for the Advection-Diffusion Equation and for Problems with Discontinuous Coefficients. Department of Mathematics and Statistics McGill University, Montréal Qubébec, Canada.

[8] F. Nier. Remarques sur les algorithmes de décomposition de domaines. In séminaire EDP-Ecole polytechnique 1998-99.

[9] Geneviève Raugel. Résolution numérique par une méthode d'éléments finis du problème de Dirichlet pour le laplacien dans un polygone. C.R Acad. Sc. Paris, t.286(8 mai 1978), serie A, pp. 791-794.

[10] FreeFem++, http:\\www.freefem.org

[11] P. Grisvard. Singularities in boundary value problems. Springer-Verlag, 1992. Research Notes in Applied Mathematics, RMA 22.

[12] C. Japhet. Conditions aux limites artificielles et décomposition de domaine : Méthode OO2 (Optimisée d'Ordre 2). Application à la résolution de problèmes en mécanique des fluides. Tech. Rep. 373, CMAP (Ecole Polytechnique), 1997.